

A New Correlation for Drag Coefficient of Extrudate Quadralobe Particles by CFD Simulation

S.H. Hashemabadi*, F. Mirhashemi

Computational Fluid Dynamics Research Laboratory, School of Chemical Engineering,
Iran University of Science and Technology, Tehran, Iran

Abstract

In this paper, drag coefficient of infinite quadralobe catalytic particle with non-circular cross sections has been investigated by Computational Fluid Dynamics (CFD) methods and for this purpose FEMLAB Multiphysics V2.3 based on finite element methods have been used. A new simple correlation for drag coefficient of infinite quadralobe particle has been established over the range of Reynolds numbers from 0.01 up to 1000. A comparative study has been made between the numerical results of this study and the available data in the literature. The predicted drag coefficient of infinite cylinder shows good agreement with experimental data within a converging quantitative error of less than 7% up to Reynolds number of 1000. The drag coefficient results for cross flow on infinite quadralobe particle shows higher value in comparison with cylindrical particle. In addition, influence of different number of particles (single, two, three and four particles) and orientation angle of particles on drag coefficient have been investigated.

Keywords: Drag Coefficient, Quadralobe Particle, Computational Fluid Dynamics (CFD), Packed Bed

1. Introduction

Reliable knowledge of the terminal settling velocity of particles in quiescent fluids, and the drag force on particles placed in moving fluid streams are often required for equipment design in a wide range in chemical, petrochemical, mineral, environmental and process industries. Examples are fixed, trickle and fluidized bed reactor, pollutant transport in the atmosphere, pneumatic and hydraulic conveying of coarse particles, liquid-solid separation and classification techniques, etc. [1].

For simulation of particles moving through

the fluids or flow moving over them, detailed information of the drag force acting on these particles is necessary. Basically, drag coefficient correlations are important design parameters in many phase-separators. Many relationships have been developed and presented in the literature relating the drag coefficient (C_d) as a function of Reynolds number (Re) for spherical particles. These correlations are complex and contain many arbitrary constants. Two good reviews have been published by Clift *et al.* [2] and Khan and Richardson [3] for spherical bodies drag coefficient correlations. A comparison between most of these correlations for

* Corresponding author: hashemabadi@iust.ac.ir

spheres shows relatively low deviations [4]. The steady-state free-fall conditions of isolated groups of ordered packed spheres moving through Newtonian fluids have been studied experimentally by Tran-Cong *et al.* [5].

In the case of non-spherical particles, less information can be found in the published literature [6-8]. By least squares fitting, an approximate solution to the equation of motion governing Stokes flow past a number of isolated closed bodies such as cylinders and cones was obtained by Bowen and Masliyah [9]. A number of empirical correlations have been proposed for regular polyhedrons by Pettyjohn and Christiansen [10] and Haider and Levenspiel [11]. Haider and Levenspiel [11] presented a generalized drag coefficient versus Reynolds for non-spherical particles. They used the concept of sphericity to account for the particle shape. Predictions by their correlation showed relatively poor accuracy for particles with sphericity equal to 0.67, therefore, some authors [12-15] attempted to improve the accuracy of the Haider and Levenspiel [11] correlations. Chien [12] and Hartman *et al.* [13] used the sphericity as shape factor, and a different approach was presented by Thompson and Clark [14]. These authors defined a shape factor, which is simply the ratio of the drag coefficient for the non-spherical particle to that of a sphere one, both evaluated at $Re=1000$. Two-dimensional flow around a circular cylinder located in a laminar crossflow for the Reynolds number range $10^{-4} \geq Re \geq 200$ was presented numerically by Lange *et al.* [16]. Gabitto and Tsouris [17] also reported a correlation to calculate explicitly terminal velocities for

particles of different shapes. Chhabra *et al.* [1] collected experimental results of 19 independent studies comprising several different particle shapes, including cylinders. The resulting data base consisted of 1900 experimental points covering wide ranges of physical properties and kinematic conditions. Considerable research effort has been expended in developing reliable and accurate predictive methods for estimating the drag force on the free falling velocity of particles in fluids. However, only averaged correlation of the drag coefficient for different particle shapes is available.

The laminar, two-dimensional flow around a particle located in a spatially and time constant velocity field has been of continuous interest to researchers involved in basic fluid mechanics. Because of common complexity in particles geometry, most numerical and experimental studies have investigated infinite particles such as cylinders [18]. Batchelor [19] derived an approximate expression for the drag of long cylinders with the symmetry axis both parallel and perpendicular to the flow. Compared with the flow past an infinite cylinder, there are remarkably few publications on drag force of other infinite complex particles. In addition to the viscosity of the medium, and the density of the fluid medium, drag coefficient of particle is strongly influenced by its size, shape and orientation with respect to flow direction. Indeed, the lack of unambiguous measure of shape, size and orientation during the settling of a non-spherical particle appears to be the main obstacle in developing universally applicable correlations. Currently efforts are directed at the development of a single

correlation for all shapes and orientation of non-spherical particles. Obviously, this approach tends to be less accurate than the specific shape correlation, but nonetheless appears to be more attractive from an engineering application view.

Hydro-treating catalysts come in many sizes and shapes depending on the applications and manufacturer. The size and shape of the catalyst pieces are important specifications that require quantification. Common shapes include spheres, pellets, cylinders and trilobe and quadralobe shaped pieces. Hashemabadi and Mirhashemi [20] studied numerically the drag coefficient of multilobe catalyst particles. Bazmi *et al.* [21] developed, based on slit model, a pellet scale model for calculation of drag force imposed on trilobe catalyst particles in a packed bed reactor. They proposed some corrections to the Ergun equation constants in various conditions for trilobe particles.

This work aims to predict the drag coefficient of single and multi quadralobe catalyst particles using Computational Fluid Dynamics (CFD) techniques. This special extrudate catalyst is widely used in desulphurization process. Due to the widespread usage of this process and a few studies that have been done on the quadralobe, this paper presents new drag coefficient for this particle and influence of

orientation of particles on it. To do so, the following approach is followed. First, a benchmark is performed to assess the hydrodynamic simulation capabilities of the CFD simulations. In this benchmark, the drag force of infinite circular cylinder in an infinite domain simulated. The simulation results are compared to theoretical and experimental data in existing literature in order to validate the use of the simulation method. Second, hydrodynamic simulations are performed for quadralobe particle and the correlation has been proposed for this case. Furthermore, the effect of number of particles on drag coefficient has been illustrated.

2. Governing Equation

Fig. 1 shows the geometry of extrudate quadralobe catalyst cross section. Due to the ratio of particle's length to diameter being too large, two dimensional (2D) simulation has been done. For calculation of drag coefficient of particles, the steady-state flow field and pressure field have been derived from numerical solution of continuity and Navier-Stokes motion equations:

$$\nabla \cdot (\rho \mathbf{V}) = 0 \quad (1)$$

$$\nabla \cdot (\rho \mathbf{V} \mathbf{V}) = -\nabla p + \nabla \cdot [\mu_t (\nabla \mathbf{V} + \nabla \mathbf{V}^\dagger)] \quad (2)$$



Figure 1. Geometry of quadralobe (a) industrial case, (b) simulation geometry.

The drag force is the component of the fluid force acting on a particle in the streamwise (x) direction and normal (y) direction to the streamwise direction, F_d , and it was computed by integrating the pressure and viscous stresses over the surface of a particle:

$$F_d = F_{d,p} + F_{d,f} = \int_S -p ds + \int_S \tau ds \quad (3)$$

The drag force, F_d , experienced by a particle settling with a uniform velocity, U_0 , is proportional to its kinetic energy:

$$F_d = C_d A_p \left(\frac{1}{2} \rho U_0^2 \right) \quad (4)$$

Where C_d is defined in terms of drag coefficient. A_p is the projected surface area of the particle normal to the direction of its motion and ρ is the density of the fluid. Most particles of practical interest have irregular shape. A variety of empirical factors have been proposed to describe non-spherical particles and correlate their flow behavior. Most of the aforementioned studies have employed the so-called equivalent volume sphere diameter as the characteristic size and sphericity to quantify its shape. Thus, all these expressions are as follows:

$$f(\text{Re}, C_d, \varphi) = 0$$

Where Re is the particle Reynolds number and φ is the sphericity of the particle.

3. CFD Simulation

3-1. Modeling Details

The most important assumptions of the CFD model are:

- The two-dimensional steady state model was used.

- An unstructured triangular grid was used. Moreover, mesh is refined in the regions close to the particle's wall due to the higher gradients in these regions.
- The fluid was assumed incompressible because the fluid flow in packed beds has (in practice) very low Mach numbers.
- Both creppy and laminar flow regimes were studied. To do so, the Reynolds number (based on approaching velocity and equivalent particle diameter) was varied from 0.01 to 1000 to fully cover range of creppy and laminar flow.
- The model in commercial CFD package FEMLAB Multiphysics ver 2.3, which is based on the finite element method, was implemented.

Fig. 2 illustrates four different computational domains A) infinite cylindrical particle, B, C and D different number of infinite quadralobe particle. All particles are subjected to the following boundary conditions:

- At inlet: uniform velocity
- At outlet: pressure outlet
- At bottom and top: Symmetry boundary
- At particle surface: No slip condition

3-2. Computational domains

As is pointed out above, due to lack of sufficient experimental data for validating drag coefficient of quadralobe particle, the drag force of infinite circular cylinder in an infinite domain was simulated (Fig. 2a).

The flow field around the cylinder is modeled in two dimensions with the axis of the cylinder perpendicular to the direction of flow. The cylinder is modeled as a circle and a rectangular flow domain is created around the cylinder (Fig. 2a). The upstream and

downstream lengths are 15 and 30 times the diameter of the cylinder, respectively. The width of the flow domain is 20 times the diameter of the cylinder. Similar to cylindrical particle, single quadralobe

particle in the same computational domain has been studied (Fig. 2b). Because of influence of particles effect on each other, two, three and four quadralobe particles have been simulated (Figs. 2c, 2d and 2e).

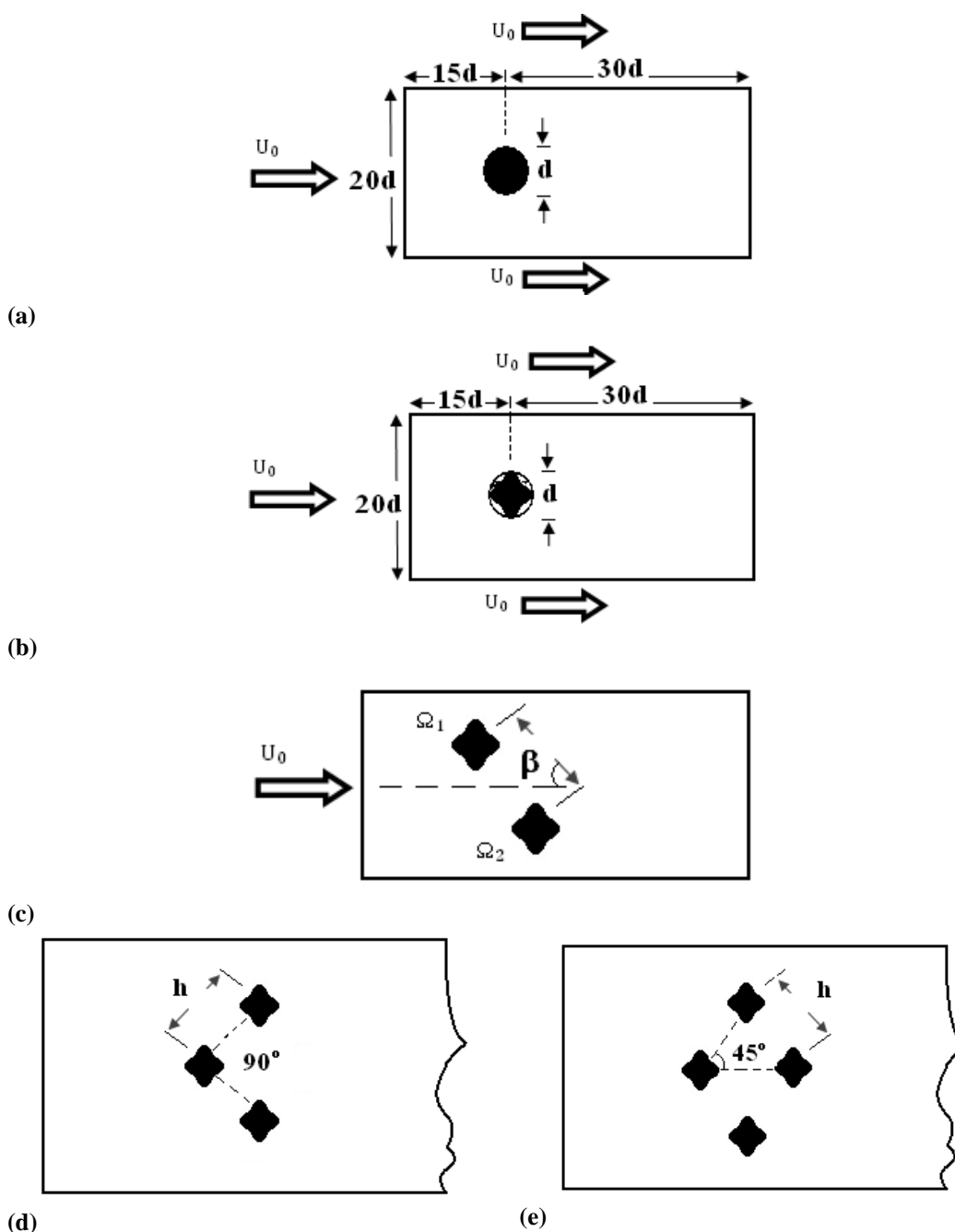


Figure 2. (a) Infinite cylindrical particle, (b) Single infinite quadralobe particle, (c) Two infinite quadralobe particles, (d) Three infinite quadralobe particles, (e) Four infinite quadralobe particles.

4. Results and discussion

4.1. Mesh Independency

For mesh independency, the drag coefficient results were verified by comparison with experimental work [22] for three different mesh densities (20000, 33000 and 50000) in different inlet velocities (see Fig. 3). The results show that predictions are better at higher mesh densities, but despite the small computational error (approx. 4%) for results in 50000 mesh density in comparison with 33000 mesh density, the computation time in this mesh density is much higher (approximately 25% more) than in the 33000 mesh density, so 33000 computational cells have been implemented in this work as the optimal mesh density in computational time and accuracy in results.

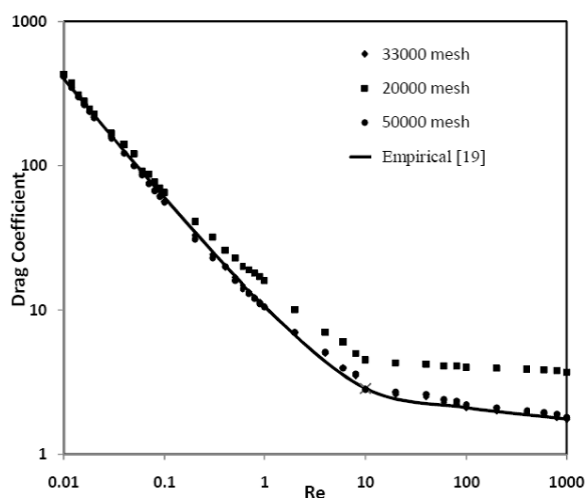


Figure 3. Variation of drag coefficient with number of cell and Reynolds number.

4-2. Validation model

All the data that is produced by CFD simulations are determined numerically and are dependent on system defined boundary conditions and user solution parameters. The first step in the solution of fluid dynamic and drag force of flow around a quadralobe

particle was to solve the problem of circular cylinder placed in an infinite domain of fluid. The main goals of this exercise were to check the mesh sensitivity and to compare the numerical solution with the correlation proposed by Schlichting and Gersten [15] and experimental data [20] in order to check the feasibility for obtaining suitable numerical results for this particle (quadralobe). Schlichting proposed the following simple correlation for drag coefficient of infinite cylinder:

$$C_d = \frac{8\pi}{Re} [\Delta - 0.87\Delta^3 + \dots] \quad Re \rightarrow 0 \quad (5)$$

Where

$$\Delta = \left[\ln \left(\frac{7.407}{Re} \right) \right]^{-1}$$

Because this work intends to study C_d of quadralobe of this range of Re , it focuses on validation of Reynolds number of 0.01 up to 1000. In fact, the CFD simulation results are presented for low and medium Reynolds numbers. Fig. 4 illustrates drag coefficient, denoted by C_d as a function of Re number. The CFD results have better agreement than Schlichting correlation in low Reynolds number. On the other hand, whereas Schlichting correlation is not appropriate, the predicted drag coefficient is in good agreement with experimental data within a converging quantitative error less than 7% up to Reynolds number of 1000. With this reasonable error it can be concluded that the mesh and numerical solution is suitable for prediction of quadralobe drag coefficient.

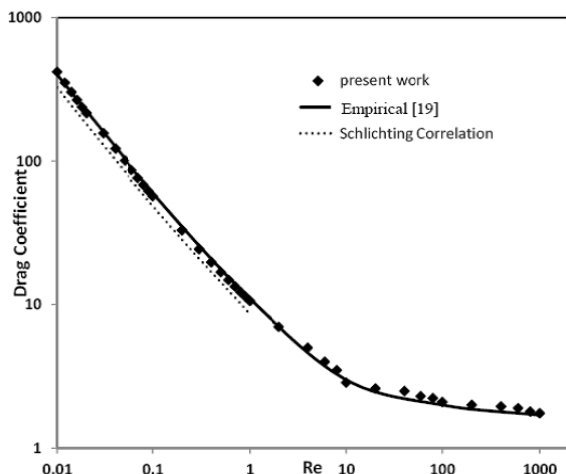


Figure 4. Measured drag coefficient, C_D , versus Reynolds number, Re .

4-3. Drag coefficient of quadralobe particle

Fig. 1 shows the geometry of quadralobe. It should be mentioned that this particle has special geometry because its lobe's size is different on both sides. The corresponding set of data for quadralobe and cylinder is shown in Fig. 5. As Fig. 5 shows, at a given Re number, the values of drag coefficient for this particle are higher than the ones for cylinder. This dissension is higher when Reynolds number increased. The effect of each lobe and the departure of particle shape from sphericity can be the reason for this difference. Furthermore, the strong force that flows with special angle involved in each lobe is different. This leads to the conclusion that the structure of lobes and therefore, sphericity is an important parameter that characterizes the settling of irregular particles. Owing to dependency of drag coefficient of this particle to its lobe size and orientation in flow domain, with regard to the sphericity directly, this model has been simulated for different sphericity. These results have been calculated for drag coefficient of quadralobe (Fig. 6) in order to

correlate an equation. According to the results, shown in Fig. 6, a correlation formula for C_d has been obtained which relates to the Reynolds number and the sphericity (ϕ) as parameters for drag force of quadralobe particle. Restrictions of applicability in terms of Re are given for these correlations. Following the trend observed in Figs. 5 and 6, two correlations of drag coefficient of quadralobe for corresponding set of CFD data are shown in Eqs. (6) and (7). As it is seen, Eq. (6) has been inspired by Schlichting correlation (Eq. 5):

$$C_d = \frac{41.66\pi\sqrt{\phi}}{Re} \left[\ln\left(\frac{7.407}{Re}\right) \right]^{-1} \quad 0.01 < Re < 0.5 \quad (6)$$

$$C_d = \frac{9.38}{Re} + 2.504 \exp(-0.0501\phi) \quad 0.5 < Re < 1000 \quad (7)$$

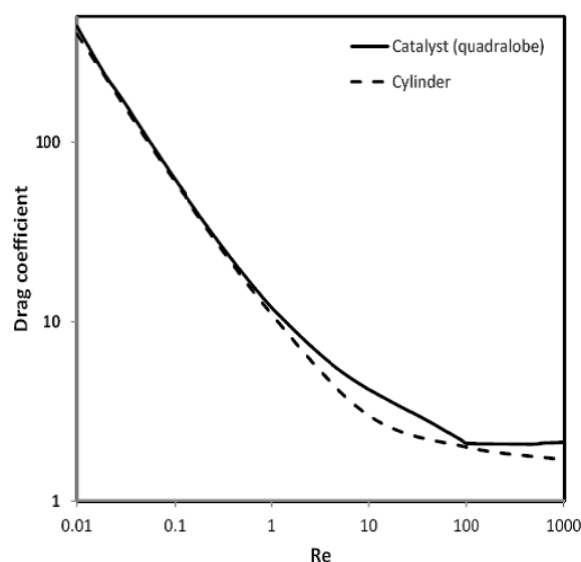


Figure 5. Comparison between the drag coefficient of circular cylinder and infinite quadralobe.

Fig.7 depicts the CFD calculated values of drag coefficient (C_d) versus the predicted

values by the above equations, over the range of $0.01 < Re < 1000$. It is observed that all the points are very close to a line at 45° (shown by the dashed line). This implies that there is good agreement between CFD data and the new correlation function. The average deviation is only about 5%.

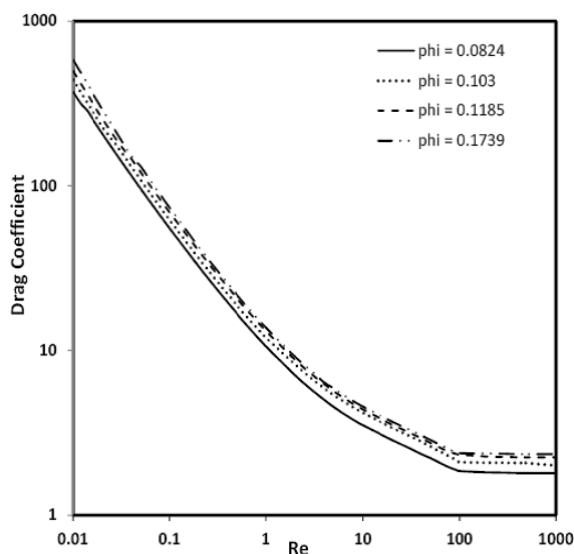


Figure 6. Variation of particle drag coefficient with different sphericity.

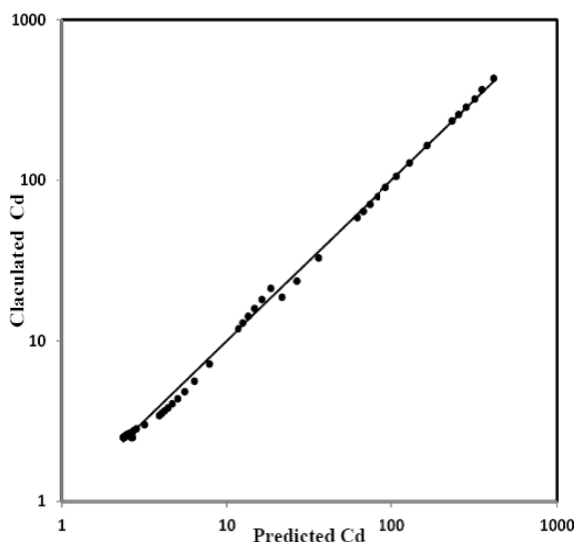


Figure 7. Comparison between CFD drag coefficient and the correlation.

4-4. Influence oriented angle of particles

In this section, the effect of angled particles toward each other on drag coefficient is considered. First, an attempt was made to resolve two-particle problem as shown in Figure (2C). In this problem, influence of swirl angle of particle Ω_1 (β) on drag force of particle Ω_2 is illustrated. Fig. 8 indicates the results of affected particle (Ω_2) drag coefficient to single particle drag coefficient ratio (C_d/C_d^*) against Reynolds number in terms of angle with the horizon (β). In this case the ratio of two particles distance (h) to equivalent diameter of quadralobe particle (d) is equal to two. It is interesting to see that the value of C_d/C_d^* at different Reynolds numbers, Re , increase with β . As it is seen in Fig. 8, in general, with increasing β from 0° to 270° , drag coefficient is decreased. There is an exception in this trend at 45° . Only at high Reynolds numbers ($Re > 0.5$), in case of $\beta = 45^\circ$, it is found that the drag coefficient for particle Ω_2 is enhanced. This effect, as a result of the situation of particles towards each other, is attributed to high velocity gradient between particle and the fluid. The effect of lobe structure can be the reason for this exception. Furthermore, the drag coefficient of particle Ω_2 at $\beta = 0^\circ$ is much stronger than that at $\beta = 270^\circ$. When particle Ω_1 is placed in back of particle Ω_2 ($\beta = 270^\circ$) there is an obstacle for fluid. Thus, drastic reduction has been created.

In order to understand the influence of particles arrangement on flow field, the velocity contours for two particles with different angles ($\beta = 0^\circ, 45^\circ, 90^\circ$) are shown in Fig. 9. As it is shown, the flow pattern changes considerably in each angle, therefore, drag coefficient changes too. In

45° angle, it is observed that, gradient velocity and drag force around particles are more complex than gradient velocity in the other two arrangements, this causes a complicated trend to be observed in this case.

4-5. Effect of number of particles

Figs. 2c, 2d and 2e show arrangement of two, three and four particles in infinite flow respectively. It should be noted that different arrangements can be used, but the distance between two particles is considered identical in each arrangement. Fig. 10 indicates variation of average drag coefficient when number of particles increased. As is shown, the mean drag coefficient of each arrangement decreased when number of particles increased. The only exception for this was observed at $Re > 10$, where the

calculated C_d for two particles was higher than the ones for single particle.

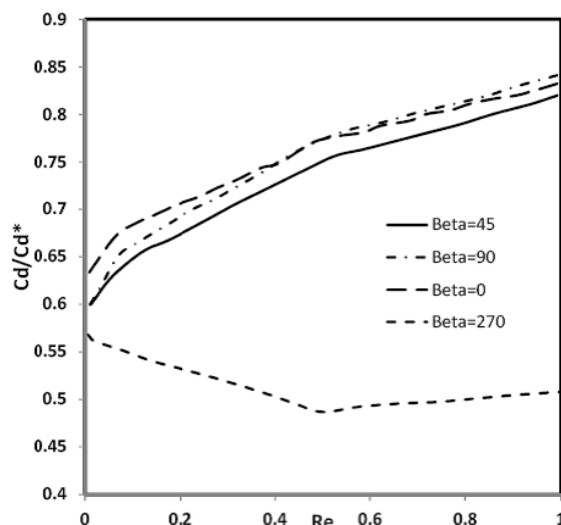


Figure 8. Computed result of relative drag coefficient C_d/C_d^* for a single quadralobe.

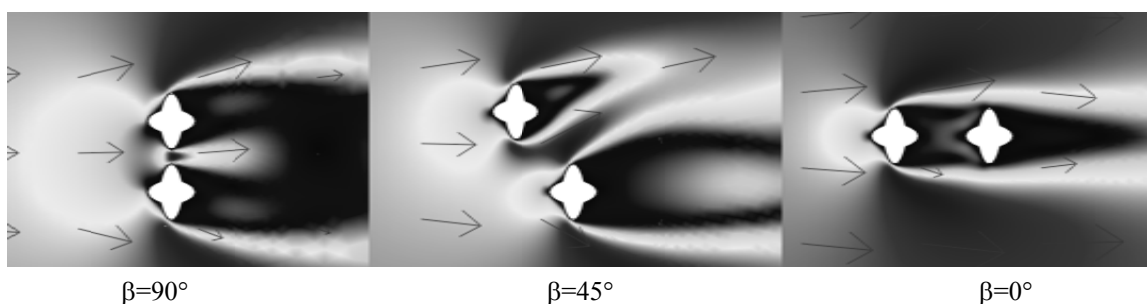


Figure 9. The velocity contour for two particles with different angle.

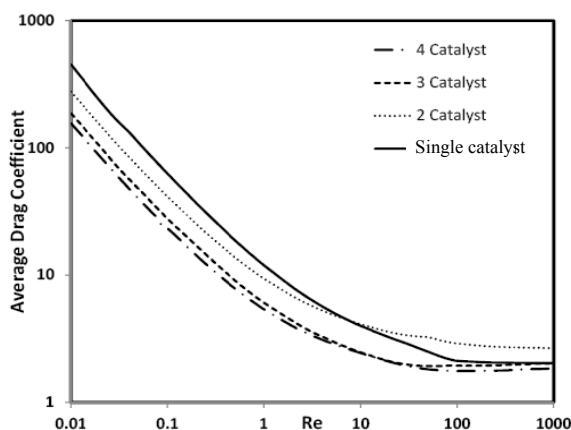


Figure 10. Variation of average drag coefficient with Reynolds number for multi particles.

4-6. Effect of distance of particles

Fig. 11 indicates variation of distance of particles to equivalent diameter ratio (h/d) when number of particles is three (Fig. 2d). At a given Reynolds number, the average drag coefficient of particles in this arrangement approaches drag coefficient of single particle when h/d is increased. Actually, the correlation for single particle drag coefficient cannot be used for particles in packed bed and the bed porosity and tortuosity have a crucial effect on bed pressure drop.

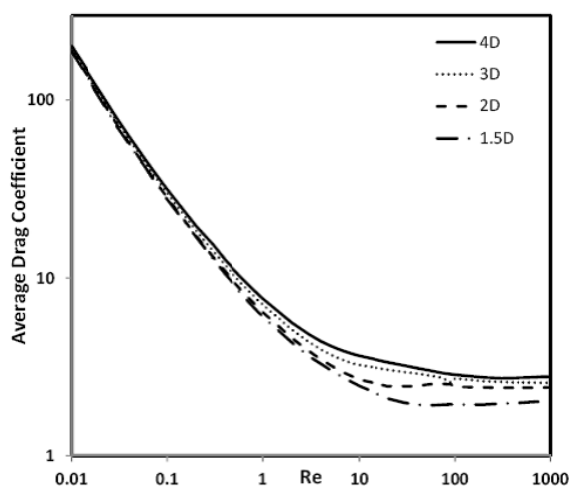


Figure 11. Variation of drag coefficient with Reynolds number in different h/D

5. Conclusions

CFD simulation has been applied to study the drag coefficient of quadralobe particles. The CFD results for cylindrical particle showed appropriate agreement in comparison with reported experimental data. Furthermore, the effect of angle of particles toward each other on drag coefficient has been investigated. As a result, in general, with increasing angle of particles from 0° to 270° relative to horizon line, drag coefficient is decreased. Moreover,

influence of particles number and distance of particles on drag coefficient were considered. With increasing number of particles, drag coefficient of each particle is decreased but due to the enhancement of the number of particles the drag coefficient moves toward a constant number and drag coefficient of each particle approaches drag coefficient of single particle while the distance between particles is increased. Finally, a new correlation is proposed for calculating values of drag coefficient (C_d) of quadralobe particles over the range of $0.01 < Re < 1000$ (The average deviation is only about 5%).

Nomenclature

A_p	Projected area (m^2)
C_d	Drag coefficient
d	Equivalent diameter (m)
h	Distance of two particles (m)
p	Pressure (Pa)
Re	Reynolds Number, $\rho U_0 d / \mu$
t	Time (s)
U_0	Free flow velocity (m/s)
V	Velocity (m/s)

Greek Symbols

β	Angle relative to horizon
Δ	Term of Eq. 5
ϕ	Sphericity
μ	Dynamic Viscosity
ρ	Density (kg/m^3)
τ	Shear Stress (pa)
Ω	Name of particle

Subscripts

1, 2	Counter
d	Drag
f	Friction
t	Turbulent

Superscript

\dagger	Transpose
-----------	-----------

References

- [1] Chhabra, R.P., Agarwal, L., and Sinha, N.K., "Drag on non-spherical particles: an evaluation of available methods", *Powder Technol.*, 10 (3), 288 (1999).
- [2] Clift, R., Grace, J.R., and Weber, M.E., *Bubbles, Drops and Particles*, Chapter 6, Academic Press, New York, (1978).
- [3] Khan, A.R., Richardson, J.F., "The resistance to motion of a solid sphere in a fluid", *Chem. Eng. Commun.*, 62, 135 (1987).
- [4] Hartman, M. and Yates, J.G., "Free-fall of solid particles through fluids", *Collect. Czech.Chem. Commun.*, 58 (5), 961 (1993).
- [5] Tran-Cong, S., Gay, M., and Michaelides E.E., "Drag coefficient of irregularly shaped particles", *Powder Technol.*, 139, 21 (2004).
- [6] Guo, X., Lin, J., and Nie, D., "New formula for drag coefficient of cylindrical particles", *Particuology*, 9 (2), 114 (2011).
- [7] Hölzer, A. and Sommerfeld, M., "New simple correlation formula for the drag coefficient of non-spherical particles", *Powder Technol.*, 184 (3), 361 (2008).
- [8] Hölzer, A., and Sommerfeld, M., "Lattice Boltzmann simulations to determine drag, lift and torque acting on non-spherical particles", *Computers & Fluids*, 38 (3), 572 (2009).
- [9] Bowen, K.O.L. and Masliyah, J.H., "Drag force on isolated axisymmetric particles in stokes flow", *Can. J. Chem. Eng.*, 45 (6), 150 (1973).
- [10] Pettyjohn, E.S. and Christiansen, E.R., "Effect of particle shape on free settling rates of isometric particles", *Chem. Eng. Prog.*, 44, 157 (1948).
- [11] Haider, A. and Levenspiel, O., "Drag coefficients and terminal velocity of spherical and nonspherical particles", *Powder Technol.*, 58, 63 (1989).
- [12] Chien, S.F., "Settling velocity of irregularly shaped particles", *SPE Drill. Completion*, 9, 281 (1994).
- [13] Hartman, M., Trnka, O., and Svoboda, K., "Free settling of nonspherical particles", *Ind. Eng. Chem. Res.* 33, 1979 (1994).
- [14] Thompson, T.L. and Clark, N.N., "A holistic approach to particle drag prediction", *Powder Technol.*, 6, 57 (1991).
- [15] Ganser, G.H., "A rational approach to drag prediction of spherical and nonspherical particles", *Powder Technol.*, 77, 143 (1993).
- [16] Lange, C.F., Durst, F., and Breuer, "Momentum and heat transfer from cylinders in laminar cross flow at $10^{-4} \leq Re \leq 200$ ", *Int. J. Heat Mass Transfer*, 41(22), 3409 (1998).
- [17] Gabitto, J.F. and Tsouris, C., "Drag coefficient and settling velocity for particles of cylindrical shape", *Powder Technol.*, 182 (2), 314 (2008).
- [18] Schlichting, K., *Gersten, Boundary Layer Theory*, 8th revised ed. Berlin, Springer, (2000).
- [19] Batchelor, G.K., *An Introduction to Fluid Dynamic*, 3rd ed., University of Cambridge, UK, P.246 (2002).
- [20] Hashemabadi, S.H. and Mirhashemi, F., "Computation of drag coefficient for infinite catalytic particles with non-circular cross sections by CFD techniques", 2nd Nat. Conf. on CFD Applications in Chemical Industries, Tehran, Iran, (2009).
- [21] Bazmi, M., Hashemabadi, S.H., and Bayat, M., "Modification of Ergun Equation for Application in Trickle Bed Reactors Randomly Packed with Trilobe Particles Using CFD Technique", *Korean J. Chem. Eng.*, 28 (6), 1340 (2011).
- [22] McCabe, W., Smith, J., and Harriott, P., *Unit Operations of Chemical Engineering*, McGraw-Hill, New York USA (2007).